

An Application of Computational Fluid Dynamics to the Hydraulic Analysis of a Water Intake Tower

Mark Wilsnack

South Florida Water Management District, West Palm Beach, Florida.

Abstract

Hydraulic engineers must sometimes perform hydraulic analyses of water control structures to evaluate system behavior under current operational demands and determine if design improvements may be needed. This paper summarizes an example of how computational fluid dynamics can be used for this purpose. A computational fluid dynamics model of a water intake tower that is connected to a pump station through a tunnel was constructed using the commercial software FLOW-3D. The model was used to evaluate head losses through the structure for a desired sustained pumping rate. The computational fluid dynamics modeling results for the intake tower indicate that if the target discharge rate is to be sustained while the upstream delivery canal stage is at its design stage, the head loss across the structure will comprise most of the head loss incurred through the water delivery system. Moreover, an examination of model output revealed certain features of the structure's hydraulic design that result in excessive losses within the tower and near the entrance of the downstream tunnel.

1 Introduction

1.1 Background

Surface water impoundments are used throughout the United States for flood control, environmental water supply storage, and storm water treatment. The design of such impoundments usually includes various hydraulic structures that regulate inflows, outflows, and stages. One relatively complex example of a system of hydraulic structures used to manage a portion of the outflows from a large storm water impoundment is shown schematically in Figure 1. For this facility, a problematic aspect of pump operations is the rapid on and off cycling that sometimes occurs during dual-pump operations that coincide with lower delivery canal stages. This cycling occurs when pump wet well levels become too low, and it typically causes the pumps to be shut down. Consequently, a hydraulic engineering evaluation of the system depicted in Figure 1 was initiated to ascertain which part(s) of the system were limiting flows to the pumps. The results of physical model tests of the pump station, along with desktop calculations of head losses incurred within the tunnel, suggest that most of the system head loss occurs within the north intake tower.

The purpose of this manuscript is to illustrate how computational fluid dynamics (CFD) was used to conduct a detailed three-dimensional hydraulic analysis of the north intake tower to better understand its effect on flow through the system. Flow through the south intake tower was not considered in this study.

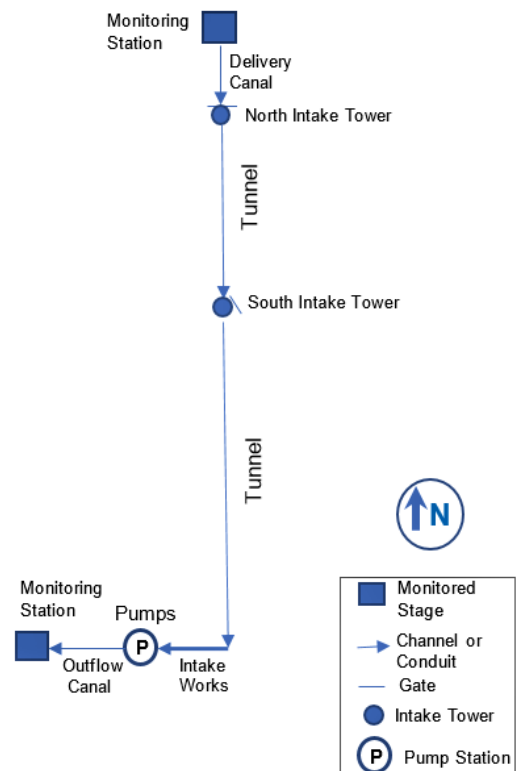


Figure 1 Schematic design of the outflow facilities.

1.2 North intake tower properties

The geometric design of the north water intake tower is provided in Figures 2 and 3. All elevations indicated are referenced to the North American vertical datum of 1988 (NAVD). It is 9.3 m high, with a 1.83 m x 1.83 m gate opening. Flow through the opening is regulated by a sluice gate with a maximum opening of 1.68 m. Water discharged through the opening drops to the bottom of the tower and flows through the tunnel to the pump station.

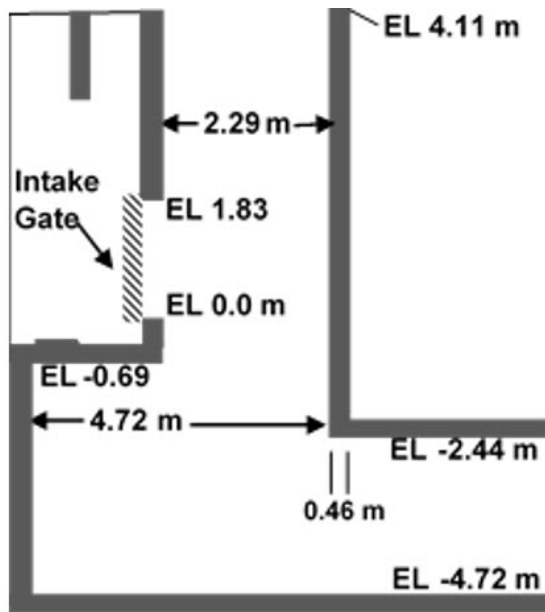


Figure 2 Cross-section dimensions of the north intake tower.

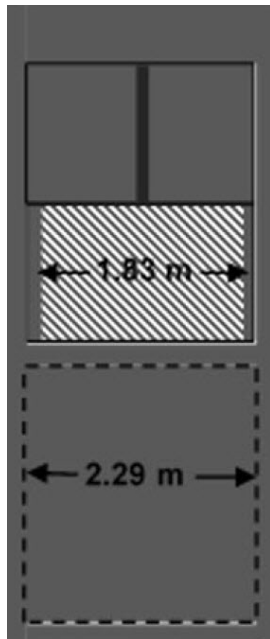


Figure 3 Front dimensions of the north intake tower.

2 Measured data

During a two-pump operation that was sustained from about 2020-10-12 20:47 h to about 2020-10-14 15:16 h, the average north intake tower head water stage was 3.14 m (based on instantaneous measurements to +0.61 cm resolution obtained through a shaft encoder with a float) while the average stage within the pump bay (just upstream of the pumps) was 2.69 m (based on instantaneous measurements obtained using a pressure sensor), resulting in an average head difference of 0.45 m during this operation. The discharge averaged approximately 5.4 m³/s during this time; however, this flow estimate is uncertain since it is based on an uncalibrated flow rating equation. The actual discharge should nonetheless be close to the nominal two-pump capacity of 5.1 m³/s. During another dual pump operation that lasted from about 2016-05-11 13:14 h–14:59 h, the average stage difference between the north intake tower head water and the pump bay was approximately 0.58 m. The accuracy of the average pump bay stage over this time window, however, is not clear since instantaneous measurements were not available during much of this time window. Furthermore, the discharge averaged about 5.15 m³/s during this time; however, this discharge estimate is also uncertain due to both the reason indicated earlier along with missing stage measurements in the pump bay.

3 CFD model setup

A computational fluid dynamics (CFD) model of the structure depicted in Figures 2 and 3 was constructed using the commercial software FLOW-3D (Flow Science, Inc., solver version 12.0.2.03) and was used to evaluate the three-dimensional flow field and head losses inherent to the design conditions.

Extensive studies on the applications of CFD to concrete spillways have been carried out by Zeng et al. (2016a; 2016b). Where applicable, the results of these studies were used to guide the current analysis.

3.1 Model domain

For practical purposes, the CFD model was limited to the most upstream portion of the seepage control system in the proximity of the north intake tower. More specifically, the portion of the system incorporated into the model included the reach of the seepage collection canal between the north intake tower and its head water monitoring station that is located approximately 41 m upstream; the structure itself as depicted in Figures 2 and 3; and the first ten hydraulic diameters of the 2.29 m x 2.29 m discharge tunnel. Figures 4(a) and 4(b) provide three-dimensional views of this portion of the system geometry. The georeferenced terrain surfaces for the upstream approach channel and overlying embankment were constructed from design information using raster generation techniques available in ArcGIS (ESRI, Inc.) All other features were incorporated into the model using the geometric primitives available in FLOW-3D.

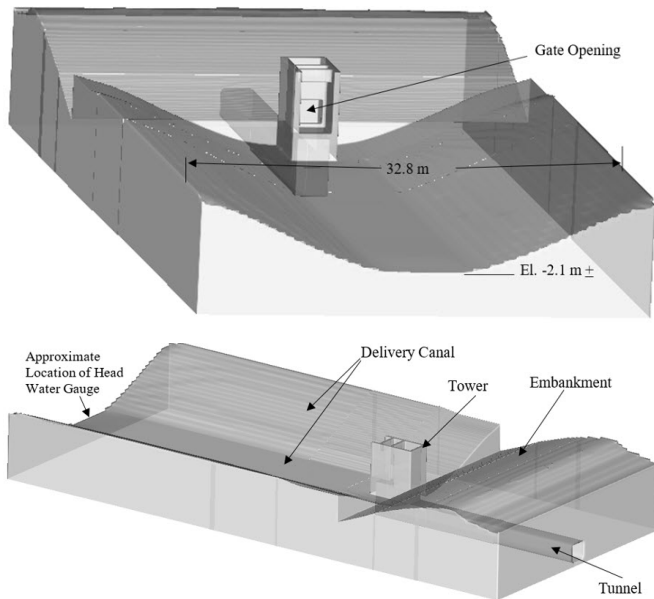


Figure 4 Three-dimensional view of the north intake tower model geometry (a, upper) facing upstream; (b, lower) facing downstream.

3.2 Numerical properties

The model was based on a numerical solution of the Reynolds-averaged Navier-Stokes (RANS) equations along with the $k-\epsilon$ turbulence transport model. A comprehensive discussion of this turbulence model is provided by Launder and Spalding (1974). They indicate that a form of this model was first proposed by Harlow and Nakayama (1968). Regarding applications, Helal et al. (2020) report that Long et al. (1991), Qingchao and Drewes (1994), and Javan and Eghbalzadeh (2013) all successfully incorporated this model into the CFD modeling of hydraulic jumps. Ge and Sotiropoulos (2005) used the $k-\epsilon$ model for the unsteady CFD modeling of flow past a bridge foundation in the Chattahoochee River. Kirkgoz et al. (2009) found that this model gave acceptable results for the CFD modeling of steady, gradually varied, supercritical flow over a round-crested spillway. Dargahi (2006) and Pedersen et al. (2018), however, found that other models they tested gave more accurate results under the conditions they studied for unsubmerged and submerged flow, respectively, over ogee spillways. When simulating flow through spillway structures using CFD, Zeng et al. (2016a) found that a number of turbulence transport models, when used in conjunction with RANS, yielded satisfactory results. In their study they found the $k-\epsilon$ model to be the most robust regarding the various initial conditions used in their simulations. Consequently, this model was used in the current study.

The volume of fluid (VOF) method (Hirt and Nichols 1981) employed by FLOW-3D was used to resolve the free water surface. A sharp air-water interface was assumed. As explained by Ferziger and Peric (1999), the VOF method introduces (to the

conservation equations for mass and momentum) and solves a transport equation for the cell volume fractions occupied by the water. The transport equation is solved throughout the entire model domain to locate the free water surface.

The numerical scheme used to solve the governing equations is the generalized minimum residual (GMRES) method. This method is based on a pressure-velocity formulation that results in coupled sets of equations that are solved iteratively by the GMRES method (Flow Science, Inc. 2020).

3.3 Boundary conditions

A constant stage of 2.65 m was set at the upstream boundary. This stage is of interest since it is the design head water stage of the north intake tower, referenced to the head water monitoring location. Discharges representing pumping rates were specified as a downstream boundary condition at the tunnel exit shown in Figure 4a. A volumetric flowrate was specified at this location so that the flow field within, and in proximity to, the tower could be evaluated under sustained pumping conditions.

A no-slip boundary condition was specified at all solid boundaries. For the concrete surfaces within the tower and tunnel, Manning's n was taken to be $0.012 \text{ s/m}^{1/3}$ while $n = 0.033 \text{ s/m}^{1/3}$ was assumed for the seepage canal wetted perimeter. As in Zeng et al. (2016a), the roughness heights applied to these surfaces were obtained from the Manning's n values through use of the relation proposed by Yen (1992).

3.4 Initial conditions

With the gate open to its maximum value of 1.68 m, it was assumed that the system was initially filled with water to an elevation or hydraulic head of 2.65 m. The gate remained in its initial position throughout the model simulation. The initial discharge was zero throughout the entire system.

3.5 Numerical mesh

A uniform cubical mesh with a resolution of 0.305 m was first applied globally to the entire model domain. This mesh was refined to 0.15 m from 12.2 m upstream of the north intake tower to 11.4 m downstream of the tower. To improve model accuracy close to the structure, a finer mesh with a cell size of 0.08 m was applied to a zone starting three meters upstream of the tower to 5.3 m downstream of the tower.

In simulating flow through gated spillways, Zeng et al. (2016a) found that near the control section for flow under a sluice gate (approximately two meters upstream and downstream of the gate), a mesh containing at least six discretization points spaced no more than 0.15 m apart was required for accurate flow estimation. Additionally, they found that for gate openings $>0.3 \text{ m}$, ignoring the boundary layer typically resulted in computed discharge errors $<0.5\%$. All of this suggests that the model discretization scheme used here should be adequate for simulating the flow field in and near the tower, and that using very small cell sizes to resolve the boundary layers should not be necessary

to achieve this purpose. The adequacy of this spatial resolution was also tested through sensitivity analysis as explained in a later section.

4 Model simulation results

Model simulations were conducted on a desktop PC with an Intel i7-8700 CPU and 64 GB of RAM. Model results for the discharge rate of 5.1 m³/s are presented here since it is the nominal capacity of a dual-pump operation. Figure 5 displays the resultant velocity distribution at this nominal discharge rate. The model results yielded a flux-averaged hydraulic head of 2.64 m over the gate opening while the corresponding hydraulic head at 10 hydraulic diameters downstream of the tower is 2.16 m. This implies that the head loss across the tower is approximately 0.48 m while the average hydraulic head within the tunnel at ten hydraulic diameters downstream from its entrance is 0.49 m lower than the stage of 2.65 m specified at the upstream boundary. Given that the tunnel is comprised of approximately 122 m of 2.29 m × 2.29 m square concrete conduit followed by approximately 67 m of 3.05 m × 3.05 m square concrete conduit, a discharge rate of 5.1 m³/s would result in a friction head loss of about 3.3 cm for the entire tunnel located downstream of the model if Manning's n is 0.012 s/m^{1/3}. Under the conditions evaluated, the first rectangular conduit will be flowing full. The second will be flowing about 80% full, although its head loss calculations assume full flow. While this assumption will somewhat over-estimate the head loss incurred within the second conduit, the head loss only amounted to about 13% of the 3.3 cm of head loss, or 4.3 mm. This is negligible. Neglecting the local head losses within the pump station intake works, all these results imply that the total system head loss is about 0.52 m. This is comparable to the aforementioned 0.45 m head loss observed in the field during a two-pump operation.

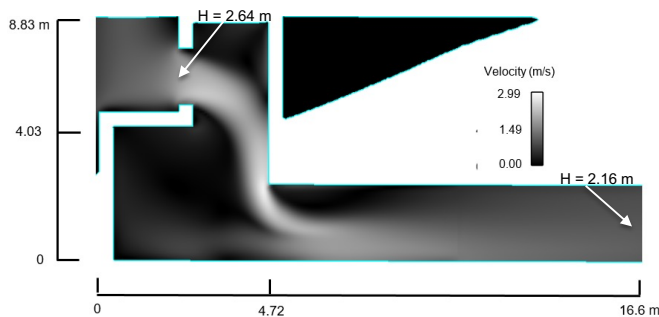


Figure 5 Velocity distribution.

Figure 5 also reveals some hydraulic features of the intake tower that require modifications. First, the tower width in the direction of flow appears to be too small since the jet passing through the gate first loses energy as it hits the opposite wall, and then subsequently loses more energy as it abruptly turns into the tunnel. Also evident is an effective reduction of flow area at the entrance of the tunnel resulting from most of the flow being concentrated within a submerged jet whose vertical

thickness is only a fraction of the tunnel height. Eddies on either side of the submerged jet are also evident. After flow enters the tunnel, it remains concentrated within the lower half of the tunnel until flow becomes more fully developed downstream.

5 Sensitivity analyses

The sensitivities of model results to surface roughness and mesh resolution were examined by evaluating the changes in model results at locations of interest resulting from changes in these model properties. Changes in the computed hydraulic head near the downstream boundary due to variations in Manning's n within expected ranges are given in Table 1. It is evident that the uncertainties in surface roughness result in downstream hydraulic head variations that are of the order of 1%. Changes of this magnitude are of little consequence to the objectives of this analysis.

Table 1 Sensitivity of downstream heads to surface roughness.

Roughness Value	Manning's n		Head at Downstream Boundary (m)	% Change from Base Simulation
	Canal	Structure		
low	0.03	0.011	2.19	1.39
base	0.033	0.012	2.16	----
high	0.035	0.013	2.13	-1.39

Also examined were variations in hydraulic head and flow rate due to variations in model discretization. In the model simulation where the spatial resolution was increased, the dimensions of each model cell in the entire model were decreased by a factor of two. In the simulation involving lower model resolution, the dimensions of each model cell within 12.2 m upstream of the tower and 11.4 m downstream of the tower were increased by a factor of two. The cell sizes elsewhere were unmodified so that the maximum cell dimension was 0.305 m. This latter resolution was maintained to avoid too much compromise in the system geometry.

Table 2 summarizes the results of this sensitivity analysis and contains the changes in hydraulic head (H) and flow rate (Q) at the locations indicated due to the changes in discretization. In particular, the percent changes in hydraulic head from the base simulation are indicated since hydraulic heads are the primary focus of the study. The simulation involving the higher resolution did not reach a steady state after more than 840 h of simulation time, so no final results were available, although fluctuations in heads and flows at the same locations indicated were small. In addition, minor fluctuations in some of the discharge rates computed in the other simulations were also evident after the system appeared to reach steady state. Nonetheless, it is apparent that the changes in computed heads due to the stated changes in model discretization are very small.

Table 2 Sensitivity of key model results to spatial discretization.

Spatial Resolution	Results at Gate Entrance			Results at 0.305 m Upstream of the Downstream Model Boundary			Run Time (h)	Comments
	H (m)	Q (cm)	% change in H from base simulation	H (m)	Q (cm)	% change in H from base simulation		
Low	2.65	2.57 ± 0.003	0.38	2.18	2.54	0.93	4.59	Small fluctuations in gate Q
Base	2.64	2.56 ± 0.009	–	2.16	2.55	–	48.49	Small fluctuations in gate Q

6 Summary and conclusions

A CFD-based hydraulic model of the gated north intake tower was constructed to evaluate head losses during system operations where higher pumping rates are sustained. The CFD modeling results for the north intake tower indicate that if a dual-pump operation were to be sustained while the upstream delivery canal stage is at 2.65 m, the head loss across the structure will be approximately 0.48 m. Since estimated head losses for the rest of the system downstream are much smaller, it was concluded that most of the head loss incurred within the entire seepage control system is due to the north intake tower structure. Moreover, an examination of model output revealed certain features of the structure's hydraulic design result in excessive losses within the tower and near the entrance of the downstream tunnel.

In consideration of these findings, it is recommended that the north intake tower be modified or replaced with a more hydraulically efficient structure so that it can sustain dual-pump operations under its design conditions. The CFD model developed as part of this study can be modified and used for this design work, after verification with additional, high quality field data. Any final design improvements should be verified through physical modeling.

Acknowledgments

The author expresses appreciation to Brian Fox and Joshua Todd of Flow Science, Inc. for their guidance and support over the duration of this project. Also acknowledged are the helpful review comments and critiques received from two anonymous reviewers.

References

Dargahi, B. 2006. "Experimental Study and 3D Numerical Simulations for a Free-Overflow Spillway." *Journal of Hydraulic Engineering* 132 (9): 899–907. [https://doi.org/10.1061/\(ASCE\)0733-9429\(2006\)132:9\(899\)](https://doi.org/10.1061/(ASCE)0733-9429(2006)132:9(899))

Ferziger, J.H., and M. Peric. 1999. *Computational Methods for Fluid Mechanics*. Berlin: Springer.

Flow Science, Inc. 2020. *FLOW-3D v. 12.0 User Manual*. Santa Fe, NM: Flow Science, Inc. <https://www.flow3d.com>

Ge, L., and F. Sotiropoulos. 2005. "3D Unsteady RANS Modeling of Complex Hydraulic Engineering Flows I: Numerical Model." *Journal of Hydraulic Engineering* 131 (9): 800. [https://doi.org/10.1061/\(ASCE\)0733-9429\(2005\)131:9\(800\)](https://doi.org/10.1061/(ASCE)0733-9429(2005)131:9(800))

Harlow, F.H., and P. Nakayama. 1968. "Transport of Turbulence Energy Decay Rate." Los Alamos, NM: Los Alamos Science Laboratory, University of California Report LA-3854. <https://doi.org/10.2172/4556905>

Helal, E., F.S. Abdelhaleem, and W.A. Elshenawy. 2020. "Numerical Assessment of the Performance of Bed Water Jets in Submerged Hydraulic Jumps." *Journal of Irrigation and Drainage Engineering*. [https://doi.org/10.1061/\(ASCE\)IR.1943-4774.0001475](https://doi.org/10.1061/(ASCE)IR.1943-4774.0001475)

Hirt, C.W., and B.D. Nichols. 1981. "Volume of Fluid (VOF) Method for the Dynamics of Free Boundaries." *Journal of Computational Physics*, 39 (1): 201–225.

Javan, M., and A. Eghbalzadeh. 2013. "2D Numerical Simulation of Submerged Hydraulic Jumps." *Applied Mathematical Modelling*. 37 (10): 6661–9. <https://doi.org/10.1016/j.apm.2012.12.016>

Kirkgoz, M.S., M.S. Akoz, and A.A. Oner. 2009. "Numerical Modeling of Flow Over a Chute Spillway." *Journal of Hydraulic Research*, 47 (6): 790–7. <https://doi.org/10.3826/jhr.2009.3467>

Lauder, B.E., and D.B. Spalding. 1974. "The Numerical Computation of Turbulent Flows." *Computer Methods in Applied Mechanics and Engineering*. 3 (2): 269–89.

Long, D., N. Rajaratnam, P. Steffler, and P. Smy. 1991. "A Structure of Flow in Hydraulic Jumps." *Journal of Hydraulic Research* 29 (2): 207–18. <https://doi.org/10.1080/00221689109499004>

Pedersen, Ø., G. Fleit, E. Pummer, B.P. Tullis, and N. Rütther. 2018. "Reynolds-Averaged Navier-Stokes Modeling of Submerged Ogee Weirs." *Journal of Irrigation and Drainage Engineering* 144 (1): 04017059. [https://doi.org/10.1061/\(ASCE\)IR.1943-4774.0001266](https://doi.org/10.1061/(ASCE)IR.1943-4774.0001266)

Qingchao, L., and U. Drewes. 1994. "Turbulence Characteristics in Free and Forced Hydraulic Jumps." *Journal of Hydraulic Research* 32 (6): 877–98. <https://doi.org/10.1080/00221689409498696>

Yen, B.C. (ed.). 1992. "Channel Flow Resistance: Centennial of Manning's Formula." Highlands Ranch, CO: Water Resources Publications.

Zeng, J., L.Q. Zhang, M. Ansar, E. Damsis, and J.A. Castro-Gonzalez. 2016a. "Applications of Computational Fluid Dynamics to Flow Ratings at Prototype Spillways and Weirs I: Data Generation and Validation." *Journal of Irrigation and Drainage Engineering* 143 (1): 04016072. [https://doi.org/10.1061/\(ASCE\)IR.1943-4774.0001112](https://doi.org/10.1061/(ASCE)IR.1943-4774.0001112)

Zeng, J., L.Q. Zhang, M. Ansar, E. Damisse, and J.A. Castro-Gonzalez. 2016b. "Applications of Computational Fluid Dynamics to Flow Ratings at Prototype Spillways and Weirs II: Framework for Planning, Data Assessment, and Flow Rating." *Journal of Irrigation and Drainage Engineering* 143 (1): 04016073. [https://doi.org/10.1061/\(ASCE\)IR.1943-4774.0001113](https://doi.org/10.1061/(ASCE)IR.1943-4774.0001113)